International Research Journal of Engineering and Technology (IRJET) e-ISSN: 2395-0056
Volume: 06 Issue: 03 | Mar 2019 www.irjet.net p-ISSN: 2395-0072

ENHANCING THE EFFICIENCY OF LICENCED SPECTRUM SHARING IN 5G HETEROGENEOUS NETWORKS

Michael Joseph Shundi[1], Ibrahim Iddi[2] Grace Gregory Mihuba[3] Toshtemirov Adkhamjon[4]

[1,3,4]*Student, School of Information and Communication Engineering, University of Science and Technology Beijing, Beijing, China*
[1,/2]*Instructor/Assistant Lecturer, Arusha Technical College, P.O. Box 296, Arusha, Tanzania*
[2]*Student, School of Electronics and Information Processing, Beihang University, Beijing, China*

Abstract - *Spectrum frequency is the most fundamental drive to communication networks; however its availability is limited. The underutilization of the licensed spectrum and the upcoming evolution of communication networks to support mega fast broadband services has led to a great scarcity and henceforth a great need of the spectrum frequency. This scarcity put an emphasis on the efficient usage of spectrum frequency. The Spectrum sharing between heterogeneous networks is recently being considered to be solution to the problem of scarcity of the spectrum frequency in the future wireless network (i.e. 5G). In this paper we discussed the spectrum sharing between multiple-input multiple-output (MIMO) radar and MIMO cellular network. Spectrum sharing algorithms are designed with consideration of MIMO radar as the primary user (PU) and cellular network as the secondary user (PU). Using the projection method, the radar signals are projected in the null space of interference channel between radar and cellular network using the interference-channel-selection algorithm in order to mitigate interference from the radar. On the other hand, we addressed the problem of target detection by radars that project waveform onto the null space of interference channel in order to mitigate interference to cellular systems. The simulation results are presented to show the performance of the radar with regards to the interference from the cellular system.*

Keywords-*Spectrum frequency, MIMO, Spectrum sharing, MIMO Radar. Interference, Cellular communication network, Radar signal. Null-space projection (NSP), Beampattern(s)*

1. INTRODUCTION

Spectrum frequency is the most significant resource for wireless communication networks but its availability is limited. The rapid growth of mobile communication networks to support a wide range of mega fast broadband services has led to a big capacity demand of the spectrum frequency[1]. The scarcity of spectrum frequency has headed to a new stimulus to search for a prominent solutions to make the most efficient use of scarce licensed frequency band in a shared mode. Spectrum sharing will enhance spectrum utilization efficiency and also save cost to the users of the spectrum[2]

1.1 Spectrum Sharing Between Radar and Cellular Communication Network

Spectrum sharing between radar and commercial cellular communication system is an immerging research area aiming to acquire more spectrum frequency to meet the high demand of this valuable resource for the upcoming growth of wireless communications. The great concern in this case is interference mitigation from the secondary user (SU) to the primary user (PU)[3]. There are number of ways which can be used to achieve spectrum sharing between radar and communication system, but in this paper we will mostly focus on: shaping the radar waveform to mitigate interference from the communication system and beamforming: where by radar signal beam can be projected to the null space interference channel to mitigate the interference between the players (ie. Radar and cellular communication network)

1.2 System Model

The system model includes; MIMO radar, target model/channel, orthogonal waveforms, interference channel, and cellular system model. Connectively, modeling and statistical assumptions and RF environment will be discussed.

1.2.1 Radar

In this paper we consider using a MIMO radar with M transmit-receive antennas. The MIMO radar antennas are spaced on the order of half the wavelength. Other classified MIMO radar have a widely spaced where antenna elements are widely spaced which results in improved spatial diversity[4] . However, the MIMO radar with antennas spaced in the order of half wavelength gives better spatial resolution and target parameter identification as compared to the widely-spaced radar[5].

1.2.2 Target

The target considered here is defined as targets having a scatterer with infinite spatial extent. This assumed model is good and is mostly used in radar theory for the case when radar elements are co-located and there is a large distance between the radar array and the target as compared to inter-

element distance [6]. Thus signal reflected from the target with unit radar cross-section (RCS) is represented numerically by the function Dirac delta.

1.2.3 Signal Model

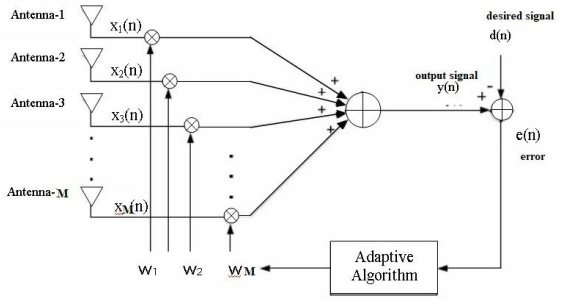

Figure 1: Uniform Linear Array (ULA) diagram **[7]**

Let the signal transmitted from the M-element MIMO radar array be **x**(t) defined as;

$$X(t) = [x_1(t)e^{-i\omega ct} x_2(t)e^{-i\omega ct} \dots . x_M(t)e^{-i\omega ct}]^T \text{..(1)}$$

Where $x_k(t)e^{-i\omega ct}$ is the baseband signal from the k^{th} transmit element, ω_c is the carrier angular frequency, $t \in [0, T_o]$, with T_o being the observation time. The transmit steering vector is defined as;

$$a_T(\theta) \triangleq [e^{-i\omega c \tau T_1(\theta)} \; e^{-i\omega c \tau T_2(\theta)} \dots . e^{-i\omega c \tau T_M(\theta)}]^T \text{..(2)}$$

Then, the transmit-receive steering matrix can be written as

$$\mathcal{A}(\theta) \triangleq a_R(\theta) a_T^T(\theta) \text{.....(3)}$$

Since, we are considering **M** transmit and receive elements, we define $a(\theta) \triangleq a_T(\theta) \triangleq a_R(\theta)$. The signal received from a single target, in far-field with constant radial velocity $\mathbf{v_r}$ at an angle θ can be written as

$$y(t) = \alpha e^{-iwDt} \mathcal{A}(\theta) x(t - \tau(t)) + \mathbf{n}(t) \text{.....(4)}$$

Where $\tau(t) = \tau T_k(t) + \tau R_l(t)$ present the sum of propagation delays between the target and the **k**th transmit element and the **l**th receive element, respectively; $\boldsymbol{\omega_D}$ is the Doppler frequency shift, α is the complex path loss including the propagation loss and the coefficient of reflection, and **n**(t) is the zero-mean complex Gaussian noise.

1.2.4 Assumptions for Modeling

The following assumptions about the signal model are made to keep the analysis tractable:

i)Due to the far-field assumption, the path loss α is assumed to be identical for all transmit and receive elements, [8].
ii) **θ** is the azimuth angle of the target.
iii) After the range-Doppler parameters compensation, we can simplify Equation (4) as

$$y(t) = \alpha \mathcal{A}(t) x(t) + \mathbf{n}(t) \text{.....(5)}$$

1.2.5 Statistical Assumptions:

The following assumptions are made for the received signal model in Equation (5):

i) θ and α are unknown parameters representing the target's direction of arrival and the complex amplitude of the target, respectively.
ii) **n**(t) is independent noise vector, zero-mean complex Gaussian with known covariance matrix $R_n = \sigma_n^2 I_M$, i. e. , $n(t) \sim \mathcal{N}^c(O_M, \sigma_n^2 I_M)$, where $\mathcal{N}^c$ represent the complex Gaussian distribution.
iii) From the assumptions above, the received signal model in Equation (5) has independent complex Gaussian distribution, i.e.

$$y(t) \sim \mathcal{N}^c(\alpha \mathcal{A}(\theta)\mathbf{x}(t), \sigma_n^2 \mathbf{I_M} \text{.....(6)}$$

1.2.6 Orthogonal Waveforms:

We consider orthogonal waveforms transmitted by MIMO radars, i.e.,

$$R_x = \int x(t) x^H(t) dt = \mathbf{I_M} \text{.....(7)}$$

Transmitting orthogonal signals gives MIMO radar advantages in terms of digital beamforming at the transmitter in addition to receiver, enhanced angular resolution, prolonged array aperture in the form of virtual arrays, improved number of resolvable targets, lower side lobes , and lower probability of intercept as compared to coherent waveforms[8].

1.2.7 Communication System

A MIMO cellular system is considered in this paper, with number of base stations =**K**, each equipped with $\mathbf{N^{BS}}$ transmit and receive antennas, with i^{th} BS supporting $\mathcal{L}_i^{UE}$ user equipment (UE). The UEs are also multi-antenna systems with N^{UE} transmit and receive antennas. If $\mathbf{S_j^{UE}(t)}$ is the signals transmitted by the **j**th UE in the i^{th} cell, then the received signal at the **i**th BS receiver can be written as

$$r_i(t) = \sum_j H_j^{N^{BS} \times N^{UE}} S_j^{UE}(t) + w(t) \quad 1 \le j \le \mathcal{L}_i^{UE} \text{... (8)}$$

Where by **w**(t) is the additive white Gaussian noise.

1.2.8 Interference Channel

We describe the interference channel that exists between MIMO cellular base station and MIMO radar. We are considering K cellular BSs that is why our model has $\mathbf{H}_i$, i = 1, 2, . . . ,K, interference channels, where the entries of $\mathbf{H}_i$ are denoted by

$$H_i \triangleq \begin{bmatrix} h_i^{(1,1)} & \dots & h_i^{(1,M)} \\ \vdots & \ddots & \vdots \\ h_i^{(N^{BS},1)} & \dots & h_i^{(N^{BS},M)} \end{bmatrix} (N_{BS} \times M) \text{....(3.9)}$$

where $\mathbf{h}_l^{(l,k)}$ represents the channel coefficient from the $\mathbf{k^{th}}$ antenna element at the MIMO radar to the $\mathbf{l^{th}}$ antenna element at the $\mathbf{i^{th}}$ BS. We are assuming that elements of $\mathbf{H}_i$ are independent, identically distributed (i.i.d.) and circularly symmetric complex Gaussian random variables with zero-mean and unit-variance, thus, having a i.i.d.

1.2.9 RF Environment for Cooperation between Radar and Cellular Communication Network

It is commonly supposed that the transmitter (frequently BS) has channel state information (CSI) either by feedback from the receiver (frequently UE), in FDD systems, or transmitters can reciprocate the channel, in TDD systems[9]. In the case of radars sharing their spectrum with communications systems one-way to get CSI is that radar approximates $\mathbf{H}_i$ based on the training symbols sent by communication receivers (or BSs in this case) [10]. Alternative approach is that radar helps communication systems in channel approximation, with the aid of a low-power reference signal, and they feed back the approximated channel to radar[11]. Since, radar signal is treated as interference at communication system, we can describe the channel as interference channel and refer to information about it as interference channel state information (ICSI). In the case where military Radar shares spectrum with another military radar, ICSI can be attained by radars easily as both systems belong to military, On the other hand, when military radar shares spectrum with a communication system, ICSI can be attained by giving enticements to communication network. The greatest enticement in this scenario is null-steering and protection from radar interference. Therefore, regardless of the sharing players and (or) scenario we have ICSI for the sake of mitigating radar interference at communication network.

2. RELATED WORK

Spectrum sharing notion has recently received significant consideration from regulatory bodies and governments worldwide as it seemed to be a promising solution to the great demand of spectrum frequency during the deployment of 5G wireless networks. Observation shows that[12][13], the traffic increase in cellular wireless communications in recent years which has been driven by popularity of great number of smart devices and Internet-based applications[2], has headed to great capacity demand which as a results require a solution since the availability of spectrum frequency is limited[1][14][15][16][17][18][19][20].

For the case of radar sharing spectrum with cellular communication network a number of research has been conducted with a number of sharing scenarios has been proposed. When radar shares spectrum with a cellular communication network sharing can be achieved by a number of ways including: cooperative sensing approach where by radar allocated band can be shared with cellular communication system[[21][22][23]]; a joint communication-radar platform where by radar can do sensing and only use the unused frequencies; shaping the radar waveforms such that they do not cause interference to the communication system[24].; database aided sensing at the cellular communication network[25]; and beamforming approach adjustments can also be deployed at MIMO radar for spectrum sharing[26]. The outcome of mutual interference in the coexistence setup on radar detection and cellular communication system throughput, highlighting some non-trivial interplays and deriving useful design tradeoffs[27]. Some designing of pre-coder of a MIMO-radar spectrally-coexistent with a MIMO cellular system wich achieve spectrum-sharing with minimal interference[28]. Weather radar networked system (WRNS) with spectrum sharing among weather radar has been presented. A prototype was also implemented to experiment and explore the feasibility with real weather radar[29]. In [30] a Steepest descent opportunistic MIMO radar was presented in the sight of spectrum sharing.

3. PROPOSED MODEL

3.1 MIMO Radar – Cellular Communication Network Spectrum Sharing

Generally, existing radar fall between 3 and 100GHz of radio frequency (RF) spectrum which is also the range desirable by cellular communication network. In the following subsection we will discuss the design architecture followed by the algorithms for spectrum sharing.

3.2 Sharing Architecture

Our scenario is presented in Figure 2 where MIMO radar is share K interference channels with the cellular communication network. In view of this scenario, the received signal at the i^{th} base station (BS) receiver can be presented as;

$$r_i(t) = H_i^{N^{BS\times M}} x(t) + \sum_j H_j^{N^{BS}\times N^{UE}} S_j^{UE}(t) + w(t) \quad \text{..... 10)}$$

The aim of the MIMO radar is to map $\mathbf{x}(t)$ onto the null-space of $\mathbf{H_i}$ so that to avoid interference to the $\mathbf{i^{th}}$ BS, i.e., $\mathbf{H_i x}(t) = \mathbf{0}$, so that $\mathbf{r_i}$ (t) has Equation (8) instead of Equation (10)

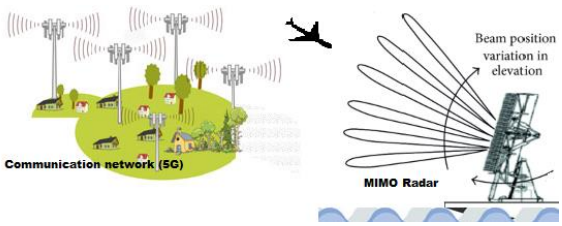

Figure 2: Spectrum sharing between MIMO radar and MIMO cellular communication Network

3.3 Sharing Algorithms for Small MIMO radar

In this section we present the performance measures of spectrum sharing between cellular communications network and MIMO radars when a MIMO radar has a smaller antenna array in comparison with a cellular base station (BS), i.e., $M_T \leq N_R$. We consider cellular system with K BSs. The MIMO radar and cellular communication network share K interference channels, i.e., $\mathbf{H_i}$, i = 1, 2. . . K. We project the radar signal onto the null space of interference channel between the MIMO radar and cellular communication system using the proposed algorithm for interference-channel-selection, aiming to have zero interference from the MIMO radar. Then interference channel with the maximum null space is selected, i.e., $\text{argmax}_{1\leq i\leq K}\dim[\mathcal{N}(\mathbf{H_i})]$ and project the radar signal onto the null space of this channel. The proposed sharing algorithm causes minimum loss in radar performance by wisely selecting the interference channel and at the meanwhile safeguards the i^{th} cell BS from the radar interference.

3.3.1 Performance Measures

Crame`r Rao bound (CRB) and maximum likelihood (ML) are chosen to approximate the angle of arrival of the target as our performance measures for the MIMO radar. Our aim is to study the degradation in the approximation of the angle of arrival of target due to null-space projection of the radar waveforms. The CRB for a single target, no-interference scenario, is as denoted in [8].

$$\text{CRB} = \frac{1}{2\text{SNR}}\left(M_R \dot{a}_T^H(\theta)R_x^T\dot{a}_T(\theta) + a_T^H(\theta)R_x^T a_T(\theta)\|\dot{a}_R(\theta)\|^2 - \frac{M_R\,|a_T^H(\theta)R_x^T a_T(\theta)\,|^2}{a_T^H(\theta)R_x^T a_T(\theta)}\right)^{-1}$$

.. ...11)

and the **ML** for the scenario of no interference and a single target can be presented as in [8]

$$(\check{\theta}, \check{\tau}_r, \check{\omega}_D)_{ML} = \underset{\theta, \tau_r, \omega_D}{\text{argmax}} \frac{|a_R^H(\theta)E(\tau_r,\omega_D)a_T^*(\theta)\,|^2}{M_R a_T^H(\theta)R_x^T a_T(\theta)} \ldots (12)$$

Where $\dot{a}_R(\theta) = \frac{da_R(\theta)}{d\theta}$

$$\dot{a}_T(\theta) = \frac{da_T(\theta)}{d\theta}$$

$$\mathbf{R_x} = \int_{T_0} X(t)X^H(t)\,dt$$

$$E(\tau_r, \omega_D) = \int_{T_0} y(t)\,X^H(t-\tau_r)e^{j\omega_D t}dt$$

τ_r is the propagation delay, two-way, between the target and the reference point, and ω_D is the Doppler frequency shift. Beampattern is a measure of beamformer's response to a target at direction θ given by, as in [8], direction θ given by, as in [8],

$$G(\theta, \omega_D) = \Gamma \frac{|a_T^H(\theta)R_x^T a_T(\theta_D)\,|^2}{a_T^H(\theta_D)R_x^T a_T(\theta_D)} \frac{|a_R^H(\theta)a_R(\theta_D)}{M_R} \ldots\ldots(13)$$

where Γ the normalization constant and θ_D is represents the digital steering direction of the main beam.

3.3.2 Interference-Channel-Selection Algorithm

We propose interference-channel-selection algorithm, denoted as **Algorithm 1**, which will be used to select interference channel onto which signals of radar are projected using Null Space Projection (NSP) approach, (i.e. **Algorithm 2**). We assumed that there exist K interference channels, i.e., $\mathbf{H_i}$, i = 1, 2, . . . ,K, between the MIMO radar and the cellular communication system and the best interference channel we aim to select is defined as

$$i_{max} \triangleq \underset{1\leq i\leq K}{\text{argmax}}\,\dim[\mathcal{N}(H_i)]$$

$$H_{Best} \triangleq H_{i_{max}}$$

And we aim to mitigate the worst channel, demarcated as

$$i_{min} \triangleq \underset{1\leq i\leq K}{\text{argmin}}\,\dim[\mathcal{N}(H_i)]$$

$$H_{Worst} \triangleq H_{i_{min}}$$

Where null space of $\mathbf{H_1}^{N_R\times M_T}$ is given as

$$\mathcal{N}(H_i) \triangleq \{x \in \mathbb{C}^{M_T} : H_i x = 0\}$$

and then null of $\mathbf{H_1}^{N_R\times M_T}$ is given as

$$\text{null } H_i \triangleq \dim[\mathcal{N}(\mathbf{H_1})]$$

where 'dim' is the number of linearly independent columns in null space of $\mathbf{H_1}^{N_R\times M_T}$. At the MIMO radar, we approximate the channel state information (CSI) of the K interference channels using a blind null-space learning algorithm . The null space of these K interference channels are calculated via **Algorithm 2**. **Algorithm 1 on** receiving null space of interference channels, it make a selection of a channel with the maximum null space as the best choice, (i.e., $\tilde{H}$ **)** and sends it to **Algorithm 2** for NSP of radar signals.

Algorithm 1: Algorithm for Interference-Channel Selection

Loop
for i=1: K do
Estimate CSI of $\boldsymbol{H_i}$
Send $\boldsymbol{H_i}$ to Algorithm (2) for null space computation

$dim[\mathcal{N}(H_i)]$
Receive the from Algorithm(2)
end for

$$i_{max} = \underset{1 \le i \le K}{argmax}\, dim[\mathcal{N}(H_i)]$$

Find

$$\tilde{H} = H_{i_{max}}$$

Set as the candidate interference channel

$\tilde{H}$
Send to Algorithm 2to get NSP waveform
end loop

After achieving CSI estimation of **K** interference channels, from **Algorithm 1**, we then find null space of each $\mathbf{H}_1^{N_R \times M_T}$ using **Algorithm 2**. This step is performed using the singular value decomposition (SVD) theorem according to our modified-NSP projection algorithm, as shown in Algorithm 2. For the complex **i**th interference channel matrix the SVD is given as

$$\mathbf{H}_1^{N_R \times M_T} = \mathbf{U}_1 \sum_1^{N_R \times M_T} \mathbf{V}_1^{H}$$

$$= \mathrm{U_i} \begin{pmatrix} \delta 1 & 0 & 0 & 0 \\ 0 & \delta 2 & 0 & 0 \\ 0 & 0 & \ddots & 0 \\ 0 & 0 & 0 & \delta_j \epsilon \min(N_R, M_T) \end{pmatrix} \mathbf{V}_1^{H}$$

where **U**i is the complex unitary matrix, **Σ**i is the diagonal matrix of singular values, and $\mathbf{V}_1^{H}$ is the complex unitary matrix In Algorithm 2, we set a threshold σ and select singular values below the threshold value for the sake that . If the SVD analysis do not yield any zero singular values we resort to a numerical approach to calculate null space. Thus, the number of singular values lower than the threshold serves as the dimension of null space.

Algorithm 2: Modified-Null-Space Projection(NSP)

If H_i is received from Algorithm 1 **then**

Perform SVD on H_i (i.e. $H_i = U_i \sum_i V_i^H$)

If $\delta \neq 0$ (i.e. j[th] singular value of $\sum_i$) **then**

$$dim[\mathcal{N}(H_i)] = 0$$

Use pre-specified threshold δ

$$\text{for j} = 1 : min(N_R, M_T)\ \textbf{do}$$

if $\sigma_j < \delta$ then

$$dim[\mathcal{N}(H_i)] = dim[\mathcal{N}(H_i)] + 1$$

Else

$$dim[\mathcal{N}(H_i)] = 0$$

end if
end for
else

$dim[\mathcal{N}(H_i)]$ = Number of zero singular values

end if

send $dim[\mathcal{N}(H_i)]$ to **Algorithm 1**

end if

If $\tilde{H}$ received from Algorithm 1 **then**

Perform SVD on $\tilde{H} = U \sum V$

If $\sigma \neq 0$ then

Use pre-specified threshold δ

$\delta_{null} = \{\}$ { An empty set to collect δs below threshold σ}

$$\text{for j} = 1 : min(N_R, M_T)\ \textbf{do}$$

if $\sigma_j < \delta$ **then**

Add σ_j to σ_{null}

end if
end for

$\tilde{V} = \sigma_{null}$ Corresponding columns in **V**

end if

Setup projection matrix $P_{\tilde{V}} = \tilde{V}\tilde{V}^H$

Get NSP radar signal via $\tilde{X} = P_{\tilde{V}} X$

end if

After determining interference channels is determined, we then target on finding the best channel$\tilde{H}$, the one with the maximum null space, which rendering to our Algorithm 1 is given as

$$i_{max} \triangleq \underset{1 \le i \le K}{\text{argmax}}\, \dim \mathcal{N}(H_i)$$

$$\tilde{H} = H_{i_{max}}$$

Algorithm 1 sends $\tilde{H}$ to **Algorithm 2** for null-space calculation, where after **SVD** the right singular vectors corresponding to vanishing singular are collected in $\tilde{V}$ for the formation of projection matrix. After this is done, we project the radar signal onto the null space of $\mathbf{H}_{Best}$ via a

modified version of our projection algorithm[31]. The modified-NSP algorithm is given as

$P_{\check{V}} = \check{V}\check{V}^H$

The waveform of the radar projected onto null space of $\check{\mathbf{H}}$ can be presented as

$\check{X} = P_{\check{V}} X$ ..... (3.14)

By inserting the projected signal, as in Equation (14), into the Cramer–Rao bound (CRB) for the single target no interference case, Equation (11), we get the CRB for the NSP projected radar waveform as

$$CRB_{NSP} = \frac{1}{2SNR}(M_R \dot{a}_T^H(\theta) R_X^T \dot{a}_T(\theta) + a_T^H(\theta) R_X^T a_T(\theta) \|\dot{a}_R(\theta)\|^2 - \frac{M_R \, |a_T^H(\theta) R_X^T \dot{a}_T(\theta)|^2}{a_T^H(\theta) R_X^T a_T(\theta)})^{-1}$$

..(15)

Likewise, Equation (14) can be substituted in equation (12) to get the ML estimate of angle arrival for the NSP projected radar waveform as

$$(\hat{\theta}, \hat{\Gamma}_r, \hat{\omega}_D) = \underset{\theta, \Gamma_r, \omega_D}{\operatorname{argmax}} \frac{|a_T^H(\theta) \mathbf{E}(\Gamma_r, \omega_D) a_T^*(\theta)|^2}{M_R \, a_T^H(\theta) R_X^T a_T(\theta)} \text{..... (.16)}$$

For the aim of analyzing the beampattern of the NSP projected waveform we can substitute Equation (14) in Equation (13) to produce

$$G_{NSP}(\theta, \theta_D) = \Gamma \frac{|a_T^H(\theta) R_X^T a_T(\theta_D)|^2}{a_T^H(\theta_D) R_X^T a_T(\theta_D)|^2} \frac{|a_T^H(\theta) a_R(\theta_D)|^2}{M_R} \text{...(17)}$$

3.4 Spectrum Sharing Algorithms for Large MIMO Radar

The problem of target detection by radars that project waveform onto the null space of interference channel in order to diminish interference to cellular systems is addressed in this section. We consider a MIMO radar and a MIMO cellular communication network with **K** base stations (BS). We consider two spectrum sharing cases which are discussed below. The target detection performance for both waveforms is studied theoretically and via Monte Carlo simulations.

Scenario 1 ($M \ll KN^{BS}$ but $M > N^{BS}$): Consider a scenario in which a MIMO radar has a very small antenna array as compared to the combined antenna array of KBSs, i.e., $M \ll KN^{BS}$, but is larger than individual BS antenna array, i.e., $M > N^{BS}$. In this case, the possibility for the MIMO radar to simultaneously mitigate interference to all the K BSs present in the network is extremely narrow because of insufficient degrees of freedom (DoF) available

Scenario 2 ($M \gg KN^{BS}$): Consider a scenario in which a MIMO radar has a very large antenna array as compared to the combined antenna array of K BSs, i.e., $M \gg KN^{BS}$. In such a case, it is obvious the MIMO radar to simultaneously mitigate interference to all the K BSs present in the network while reliably detecting targets. This is because sufficient degrees of freedom are available for both the tasks. In such a scenario, the combined interference channel that the MIMO radar shares with K BSs in the networks is presented as$H = [H_1, H_2, H_3 \ldots . H_K]$.....(18)

3.3.1 Projection Matrix

We present formation of projection matrices for Scenario 1 and Scenario 2. Projection for Scenario 1($M \ll KN^{BS}$ but $M > N^{BS}$): We state the projection algorithm for 'Scenario 1' which projects radar signal onto the null space of interference channel $\mathbf{H_i}$. Win an assumption of, the MIMO radar has channel state information of all $\mathbf{H_i}$ interference channels, through feedback, we can perform singular value decomposition (SVD) to calculate the null space and then construct a projector matrix. We continue by first finding SVD of H_i , i.e.,

$H_i = U_i \sum_i V_i^H$ ..... (19)

Now, let us define

$\widetilde{\sum_1} \triangleq diag(\widetilde{\sigma_{1,1}}, \widetilde{\sigma_{1,2}}, \ldots, \widetilde{\sigma_{1,p}})$ ..... (20)

Where,

$p \triangleq \min(N^{BS}, M)$, and

$\widetilde{\sigma_{1,1}} > \widetilde{\sigma_{1,2}} > \cdots > \widetilde{\sigma_{1,q}} > \widetilde{\sigma_{1,q+1}} = \widetilde{\sigma_{1,q+2}} = \cdots = \cdots \widetilde{\sigma_{1,p}} = 0$

are the singular values of $\mathbf{H_i}$. Next, we define

$\widetilde{\sum_1}' \triangleq diag(\widetilde{\sigma'_{1,1}}, \widetilde{\sigma'_{1,2}}, \ldots, \widetilde{\sigma'_{1,M}})$ .....(21)

Where

$\widetilde{\sigma'_{1,u}} \triangleq \begin{cases} 0, for\ u \le q, \\ 1, for\ u > q. \end{cases}$ .....(22)

Using above definitions we can now state our projection matrix, i.e.,

$P_i \triangleq V_i \widetilde{\sum_1}' V_i^H$ .....(23)

Below, we are showing two properties of a projection matrix to prove that P_i is a projection matrix;

First property: $P_i \in \mathbb{C}^{M \times M}$ is a projection matrix if and only if $P_i = P_i^H = P_i^2$.

PROOF: Let's start by proving: "$P_i = P_i^H = P_i^2$" part

Considering equation (3.23) then we have;

$P_i^H = (V_i \widetilde{\sum_1}' V_i^H)^H = P_i$.....(24)

Now squaring equation (23) we have;

$P_i^2 = V_i \tilde{\sum}_i V_i^H \times V \tilde{\sum}_i V_i^H = P_i$ .....(25)

Where, $V_i^H V_i = I$ (since they are orthogonal matrices) and $(\tilde{\sum}_i')^2 = \tilde{\sum}_i'$ (by construction). Equation (24) and (25) proves that; $P_i = P_i^H = P_i^2$

Next, we show P_i is a projection matrix by showing that if v∈ range (P_i) then

$P_i v = v$ i.e., for some w, $v = P_i w$, then

$P_i v = P_i (P_i w) = P_i^2 w = P_i w = v$.....(26)

Further to that,

$P_i v - v \in$ null (P_i), i.e.,

$P_i (P_i v - v) P_i^2 v - P_i v = P_i v - P_i v = 0$..... (27)

Hence proved.

Second property: $P_i \in \mathbb{C}^{M \times M}$ is an orthogonal projection matrix onto the null space of

$H_i \in \mathbb{C}^{N^{BS} \times M}$

PROOF: Since, $P_i = P_i^H$ we can write

$H_i P_i^H = V_i \tilde{\sum}_i V_i^H \times V_i \tilde{\sum}_i' V^H = 0$..... (28)

The results above follow by noting that: $\tilde{\sum}_i \tilde{\sum}_i' = 0$ (by construction)

For 'Scenario 1' we are dealing with K interference channels. Thus, we need to select the interference channel which results in least degradation of radar waveform in a minimum norm sense, i.e.,

$i_{min} \triangleq \underset{1 \le i \le K}{\operatorname{argmin}} \|P_i X(t) - X(t)\|_2$ .....(29)

$\check{P} = P_{i_{min}}$ ..... (30)

Afeter we have selected our projection matrix we project radar signal onto the null space of interference channel via

$\check{X}(t) = \check{P} X(t)$ ..... (31)

The correlation matrix of our NSP waveform is given as

$R_{\check{X}} = \int_{T_o} \check{X}(t)\, \check{X}^H(t)\, dt$ ..... (32)

which is no longer identity, because the projection does not preserve the orthogonality, and its rank depends upon the rank of the projection matrix.

Projection for Case 2 ($M \gg KN^{BS}$): We define the projection algorithm for 'Scenario 2' which projects radar signal onto the null space of combined interference channel **H**. The SVD of **H** is presented as

$H = U \sum V^H$ ..... (34)

Now, let us define

$\tilde{\sum} \triangleq diag(\tilde{\sigma_1}, \tilde{\sigma_2}, \dots, \tilde{\sigma_p})$ ..... (34)

Where $p \triangleq min(N^{BS}, M)$ and

$\tilde{\sigma_1} > \tilde{\sigma_2} > \cdots > \tilde{\sigma_q} > \tilde{\sigma_{q+1}} = \tilde{\sigma_{q+2}} = \cdots = \cdots \tilde{\sigma_p} = 0$

are the singular values of **H**. Next, we define

$\tilde{\sum}_i' \triangleq diag(\tilde{\sigma}_1, \tilde{\sigma}_2, \dots, \tilde{\sigma}_M$ .. (35)

Where

$\tilde{\sigma}_u \triangleq \begin{cases} 0, for\ u \le q, \\ 1, for\ u > q. \end{cases}$ ..... (36)

Using above definitions we can now define our projection matrix, i.e.,

$P \triangleq V \tilde{\sum}' V^H$ ..... (37)

It is straightforward to see that **P** is a valid projection matrix by using Properties 1 and 2.

3.4.2 Spectrum Sharing and Projection Algorithms

We explain spectrum sharing and projection algorithms for 'Scenario 1' and 'Scenario 2'.

Algorithms for Scenario 1($M \ll KN^{BS}$ but $M > N^{BS}$): For this case, the process of spectrum sharing by forming projection matrices and selecting interference channels is executed with the help of Algorithms 3 and 4. First, at each pulse repetition interval (PRI), the radar obtains ICSI of all **K** interference channels. This information is sent to Algorithm 4 for the calculation of null spaces and formation of projection matrices. Algorithm 3 process **K** projection matrices, received from Algorithm 4, to find the projection matrix which results in least degradation of radar waveform in a minimum norm sense. This step is followed by the projection of radar waveform onto the null space of the selected BS, i.e., the BS to the corresponding selected projection matrix, and waveform transmission.

Algorithm 3: Spectrum Sharing Algorithm for Scenario 1

Loop
for i=1: K **do**

Get CSI of $\mathbf{H_i}$ through feedback from the **i**th BS

Send $\mathbf{H_i}$ to Algorithm (4) for the formation of projection matrix $\mathbf{P_i}$

Receive the ith projection matrix $\mathbf{P_i}$ from Algorithm(4)

end for

Find $i_{min} = \underset{1\le i\le K}{argmin} \|\mathrm{P_i X(t)} - \mathrm{X(t)}\|_2$

$\breve{\mathrm{P}} = \mathrm{P}_{\mathrm{i}_{\min}}$ as the desired projector

Perform Null Space Projection, i.e., $\breve{\mathrm{X}}(\mathrm{t}) = \breve{\mathrm{P}}\mathrm{X}(\mathrm{t})$.

End loop

Projection for Scenario 2 ($M \gg KN^{BS}$): For this case, the process of spectrum sharing is executed with the help of Algorithms 5 and 6. First, at each pulse repetition interval (PRI), the radar obtains ICSI of all K interference channels. This information is sent to Algorithm 6 for the calculation of null space of **H** and the formation of projection matrix **P**. The projection of radar waveform onto the null space of **H** is performed by Algorithm 5

Algorithm 4: Projection Algorithm for Scenario 1

If H_i is received from Algorithm 3 **then**

Perform SVD on H_i (i.e. $H_i = U_i \sum_i V_i^H$)

Construct $\widetilde{\sum_i} = diag(\widetilde{\sigma_{i,1}}, \widetilde{\sigma_{i,2}}, \dots, \widetilde{\sigma_{i,p}})$

Construct $\widetilde{\sum_i}' = diag(\widetilde{\sigma^{-1}}_1, \widetilde{\sigma^{-1}}_2, \dots, \widetilde{\sigma^{-1}}_M)$

Setup projection matrix $P_i \triangleq V_i \widetilde{\sum_i}' V_i^H$

Send $\mathbf{P}_i$ to Algorithm 3.

end if

Algorithm 5 Spectrum Sharing Algorithm for Scenario 2

Loop

Get CSI of **H** through feedback from KBSs.

Send **H** to Algorithm 6 for the formation of projection matrix **P**.

Receive the projection matrix **P** from Algorithm 6.

Perform null space projection, i.e., $\breve{X}(t) = PX(t)$.

end loop

Algorithm 6: Projection Algorithm for Scenario 2

If **H** received from Algorithm 5 **then**

Perform SVD on **H (i.e.** $H = U\sum V^H$)

Construct $\widetilde{\sum_i} = diag(\widetilde{\sigma_1}, \widetilde{\sigma_2}, \dots, \widetilde{\sigma_p})$

Construct $\widetilde{\sum_i}' = diag(\widetilde{\sigma^{-1}}_1, \widetilde{\sigma^{-1}}_2, \dots, \widetilde{\sigma^{-1}}_M)$

Setup matrix projection $P = V\widetilde{\sum}' V^H$

Send P to Algorithm 5

end if

We develop a statistical decision test for target irradiated with the orthogonal radar waveforms and the NSP projected radar waveforms. The goal is to compare performance of the two waveforms by looking at the test decision on whether the target is present or not in the range-Doppler cell of interest.

For target detection and estimation, we proceed by constructing a hypothesis test where we seek to choose between two hypothesis: the null hypothesis H_0 which represents the case when the target is absent or the alternate hypothesis H_1 which represents the case when the target is present. The hypothesis for a single target model in Equation (5) can be written as

$$y(t) = \begin{cases} H_1: \alpha A(\theta) X(t) + n(t), & 0 \le t \le T_0, \\ H_0: n(t), & 0 \le t \le T_0. \end{cases} \quad \dots(38)$$

Since, θ and α are unknown, but deterministic, we use the generalize likelihood ratio test (GLRT). The advantage of using GLRT is that we can replace the unknown parameters with their maximum likelihood (ML) estimates. The ML estimates of α and θ are found for various signal models, targets, and interference sources in [4, 17] when using orthogonal signals. In this chapter, we consider a simpler model with one target and no interference sources in order to study the impact of NSP on target detection in a tractable manner. Therefore, we present a simpler derivation of the ML estimation and GLRT.

The received signal model in Eq. (3.5) can be written as

$$y(t) = Q(t,\theta)\alpha + n(t) \quad \dots\dots (39)$$

Where

$$Q(t,\theta) = A(\theta)X(t) \dots\dots (40)$$

We use Karhunen–Loève expansion for derivation of the log-likelihood function for estimating θ and α. Let Ω denote the space of the elements of {**y**(t)}, {**Q**(t, θ)}, and {**n**(t)}.

Moreover, let Ψ_z, z = 1, 2, . . . , be an orthonormal basis function of Ω satisfying

$$< \Psi_z(t), \Psi_{z'}(t) \geq = \int_{T_0} \Psi_z(t), \Psi^*{}_{z'}(t) = \delta_{zz'} \text{..} \quad (41)$$

where $\delta_{zz'}$ is the Krönecker delta function. Then, the following series can be used to expand the processes, {**y**(t)}, {**Q**(t, θ)}, and {**n**(t)}, as

$$y(t) = \sum_{z=1}^{\infty} y_z \Psi_z(t) \quad \ldots\ldots\ldots\ldots\ldots\ldots\ldots\ldots \quad (42)$$

$$Q(t,\theta) = \sum_{z=1}^{\infty} Q_z(\theta) \Psi_z(t) \quad \ldots\ldots\ldots\ldots\ldots\ldots \quad (43)$$

$$n(t) = \sum_{z=1}^{\infty} n_z \Psi_z(t) \quad \ldots\ldots\ldots\ldots\ldots\ldots \quad (44)$$

where y_z ,$\mathbf{Q}_z$, and $\mathbf{n}z$ are coefficients in the Karhunen–Loève expansion of the considered processes obtained by taking the corresponding inner product with basis function $\Psi_z(t)$. Thus, an equivalent discrete model of Eq. (39) can be obtained as

$$y(z) = Q_z(\theta)\alpha + n_z, \mathbf{z=1,2\ldots\ldots} \quad \ldots\ldots\ldots\ldots\ldots\ldots\ldots\ldots \quad (45)$$

For white circular complex Gaussian processes, i.e., $\mathbb{E}[\mathbf{n}(t)\mathbf{n}(t - \mathbb{T}(t))] = \sigma_n^2 \boldsymbol{I}_M \delta(\mathbb{T}(t))$, the sequence {$n_z$} is i.i.d. and $\boldsymbol{n}_z \sim \mathcal{N}^{\mathcal{C}}()_M, \ \sigma_n^2 \boldsymbol{I}_M)$. Thus, we can express the log-likelihood function as

$$L_y(\theta,\alpha) = \sum_{z=1}^{\infty}(-Mlog(\pi\,\sigma_n^2) - \frac{1}{\sigma_n^2}\|y_z - Q_z(\theta)\alpha\|^2 \ldots\ldots\ldots\ldots \quad (46)$$

Maximizing Equations (46) with respect to α gives

$$L_y(\theta,\alpha) = \Gamma' - \frac{1}{\sigma_n^2}(E_{yy} - e_{Qy}^H E_{QQ}^{-1} e_{Qy}) \quad \ldots\ldots(47)$$

Where

$$\Gamma' \triangleq Mlog(\pi\sigma_n^2) \quad \ldots\ldots\ldots\ldots\ldots\ldots\ldots\ldots \quad (48)$$

$$E_{yy} \triangleq \sum_{z=1}^{\infty} \|y_z\|^2 \quad \ldots\ldots\ldots\ldots\ldots\ldots\ldots\ldots \quad (49)$$

$$e_{Qy} \triangleq \sum_{z=1}^{\infty} Q_z^H y_z \quad \ldots\ldots\ldots\ldots\ldots\ldots\ldots\ldots \quad (50)$$

$$E_{QQ}^{-1} \triangleq \sum_{z=1}^{\infty} Q_z^H Q_z \quad \ldots\ldots\ldots\ldots\ldots\ldots\ldots\ldots \quad (51)$$

Note that, in Equation (47), apart from the constant Γ', the remaining summation goes to infinity. However, due to the non-contribution of higher order terms in the estimation of θ and α summation can be finite. Using the identity

$$\int_{T_0} V_1(t) V_2^H(t) dt = \sum_{z=1}^{\infty} V_{1z} V_{2z}^H \quad \ldots\ldots\ldots\ldots\ldots \quad (52)$$

For $V_i(t) = \sum_{z=1}^{\infty} V_{1z} \Psi_z(t)$, i=1,2 Equations (49) – (51) can be written as

$$E_{yy} \triangleq \int_{T_0} \|y(t)\|^2 dt \quad \ldots\ldots\ldots\ldots\ldots\ldots\ldots\ldots \quad (53)$$

$$e_{Qy} \triangleq \int_{T_0} Q^H(t,\theta) y(t) dt \quad \ldots\ldots\ldots\ldots\ldots\ldots \quad (54)$$

$$E_{QQ} \triangleq \int_{T_0} Q^H(t,\theta) Q(t,\theta) dt \quad \ldots\ldots\ldots\ldots\ldots\ldots \quad (55)$$

Using the definition of **Q**(t, θ) in Equation (40), we can write the f th element of e_{Qy} as

$$[e_{Qy}]_f = a^H(\theta_f) E^T a(\theta_f) \quad \ldots\ldots\ldots\ldots\ldots\ldots\ldots \quad (56)$$

Where

$$E = \int_{T_0} y(t) X^H(t)\, dt \quad \ldots\ldots\ldots\ldots\ldots\ldots\ldots\ldots \quad (57)$$

Similarly, we can write the f gth element of $\mathbf{E}_{\mathbf{QQ}}$ as

$$[E_{QQ}]_{fg} = a^H(\theta_f)\, a(\theta_g)\, a^H(\theta_f) R_x^T a(\theta_g) \quad \ldots\ldots (58)$$

Since, $\boldsymbol{e}_{\boldsymbol{Qy}}$ and $\mathbf{E}_{\mathbf{QQ}}$ are independent of the received signal, the sufficient statistic to calculate θ and α is given by **E**. Using Equations (56)–(58) we can write the ML estimate in matrix-vector form as

$$L_y(\hat{\theta}_{ML}) = \underset{\theta}{\operatorname{argmax}} \frac{|a^H(\hat{\theta}_{ML}) E a^*(\hat{\theta}_{ML})|^2}{M a^H(\hat{\theta}_{ML}) R_X^T a(\hat{\theta}_{ML})} \quad \ldots\ldots\ldots (59)$$

Then, the GLRT for our hypothesis testing model in Equation (38) is given as

$$L_y = \max_{\theta,\alpha}\{log f_y(y,\theta,\alpha;\mathrm{H}_1)\} - log f(y;\mathrm{H}_0) \underset{\mathrm{H}_0}{\overset{\mathrm{H}_1}{\gtrless}} \delta \quad 60)$$

Where $f_y(y,\theta,\alpha;\mathrm{H}_1)$ and $f(y;\mathrm{H}_0)$ are the probability density functions of the received signal under hypothesis $\mathrm{H}_1$and H_0, respectively. Hence, the GLRT can be expressed as

$$L_y(\hat{\theta}_{ML}) = \underset{\theta}{\operatorname{argmax}} \frac{|a^H(\hat{\theta}_{ML}) E a^*(\hat{\theta}_{ML})|^2}{M a^H(\hat{\theta}_{ML}) R_X^T a(\hat{\theta}_{ML})} \underset{\mathrm{H}_0}{\overset{\mathrm{H}_1}{\gtrless}} \delta \quad \ldots(61)$$

The asymptotic statistic of $L_y(\hat{\theta}_{ML})$ for both the hypothesis is given by [32]

$$L_y(\hat{\theta}_{ML}) \sim \begin{cases} \mathrm{H}_1 : x_2^2(\rho), \\ \mathrm{H}_0 : x_2^2, \end{cases} \quad \ldots\ldots\ldots\ldots\ldots\ldots (62)$$

where

=>$x_2^2(\rho)$ is the non-central chi-squared distributions with two degrees of freedom,
=>x_2^2 is the central chi-squared distributions with two degrees of freedom,
=>and ρ is the non-centrality parameter, which is given by

$$\rho = \frac{|\alpha|^2}{\sigma_n^2} |a^H(\theta) R_x^T a(\theta)|^2 \quad \ldots\ldots\ldots\ldots\ldots (63)$$

For the general signal model, we set δ according to a desired probability of false alarm P_{FA}, i.e.,

$$P_{FA} = P(L(y) > \delta \mid H_0) \quad \text{.....(64)}$$

$$\delta = \mathcal{F}_{x_2^2}^{-1}(1 - P_{FA}) \quad \text{.....(65)}$$

Where $\mathcal{F}_{x_2^2}^{-1}$ is the inverse central chi-squared distribution function with two degrees of freedom. The probability of detection is given by

$$P_D = P(L(y) > \delta \mid H_1) \quad \text{..... (66)}$$

$$P_D = 1 - \mathcal{F}_{x_2^2(\rho)}(\mathcal{F}_{x_2^2}^{-1}(1 - P_{FA})) \quad \text{..... (67)}$$

Where $\mathcal{F}_{x_2^2(\rho)}$ is the noncentral chi-squared distribution function with two degrees of freedom and non-centrality parameter ρ

P_D for Orthogonal Waveforms=>

For orthogonal waveforms $R_X^T = I_M$, therefore, the GLRT can be expressed as

$$L_{Orthog}(\hat{\theta}_{ML}) = \frac{|a^H(\hat{\theta}_{ML})Ea^*(\hat{\theta}_{ML})|^2}{Ma^H(\hat{\theta}_{ML})a(\hat{\theta}_{ML})} \underset{H_0}{\overset{H_1}{\gtrless}} \delta_{Orthog} \text{...(68)}$$

and the statistic of $(L(\hat{\theta}_{ML})$ for this case is

$$L_{Orthog}(\hat{\theta}_{ML}) \sim \begin{cases} H_1 : x_2^2(\rho_{Orthog}), \\ H_0 : x_2^2, \end{cases} \text{.....(69)}$$

$$\rho_{Orthog} = \frac{M^2 |\alpha|^2}{\sigma_n^2} \text{.....(70)}$$

We set δ_{Orthog} according to a desired probability of false alarm $P_{PF-Orthog}$

$$\delta_{Orthog} = \mathcal{F}_{x_2^2}^{-1}(1 - P_{PF-Orthog}) \text{.....(71)}$$

and then the probability of detection for orthogonal waveforms is given by

$$P_{D-Orthog} = 1 - \mathcal{F}_{x_2^2(\rho_{Orthog})}(\mathcal{F}_{x_2^2}^{-1}(1 - P_{PF-Orthog})) \text{.....(72)}$$

P_D for NSP Waveforms=>

For spectrum sharing waveforms $R_X^T = R_x^T$ therefore, the GLRT can be expressed as

$$L_{NSP}(\hat{\theta}_{ML}) = \frac{|a^H(\hat{\theta}_{ML})Ea^*(\hat{\theta}_{ML})|^2}{Ma^H(\hat{\theta}_{ML})R_x^T a(\hat{\theta}_{ML})} \underset{H_0}{\overset{H_1}{\gtrless}} \delta_{NSP} \text{.....(73)}$$

and the statistic $L(\hat{\theta}_{ML})$ of for this case is

$$L_{NSP}(\hat{\theta}_{ML}) \sim \begin{cases} H_1 : x_2^2(\rho_{NSP}), \\ H_0 : x_2^2, \end{cases} \text{.....(74)}$$

$$\rho_{NSP} = \frac{|\alpha|^2}{\sigma_n^2} |a^H(\theta)R_x^T a(\theta)|^2 \text{.....(75)}$$

We set δ_{NSP} according to a desired probability of false alarm P_{PF-NSP}, i.e.,

$$\delta_{NSP} = \mathcal{F}_{x_2^2(\rho_{NSP})}^{-1}(1 - P_{PF-NSP}) \text{.....(76)}$$

and then the probability of detection for orthogonal waveforms is given by

$$P_{D-NSP} = 1 - \mathcal{F}_{x_2^2(\rho_{NSP})}(\mathcal{F}_{x_2^2}^{-1}(1 - P_{PF-NSP})) \text{.....(77)}$$

4. RESULTS AND DISCUSSION

In this section we analyze the performance of spectrum sharing by analyzing the the detection ability of the MIMO radar which shares spectrum with the cellular communication network, Monte Carlo simulation is carried out using the radar parameters in Table 1.

Table 1. MIMO radar system parameters

PARAMETER	NOTATION	VALUE
Radar/Communication System RF band	-	3550 – 3650 MHz
Radar antennas	M	8, 4
Communication System Antennas	$\mathcal{N}^{BS}$	2
Carrier frequency	f_c	3.55 GHz
Wavelength	λ	8.5 cm
Inter-element antenna spacing	3 λ/4	6.42 cm
Radial velocity	V_r	2000 m/s
Speed of light	C	3×10^8 m/s
Target distance from the radar	r0	500 Km
Target angle	θ	$\hat{\theta}$
Doppler angular frequency	ω_D	$2\omega_D v_r/c$
Two way propagation delay	τ_r	2r0/c
Path loss	α	$\hat{\alpha}$

4.1 Scenario-1 Analysis

In this scenario, Monte Carlo simulation we generate K Rayleigh interference channels each with dimensions NBS × M, calculate their null spaces and construct corresponding projection matrices using Algorithm 4, the best channel is determined to perform projection of radar signal onto null space (Algorithm 3), NSP signal is transmitted, parameters θ and α estimated from the received signal, and calculate the probability of detection for orthogonal and NSP waveforms.

In Figure 3, we show the use (Algorithms 3 and 4) in enhancing target MIMO radar target detection performance when multiple BSs are subjected in detection area of radar and the radar has to consistently detect target while not interfering with cellular communication network. In this demonstration we consider a scenario with five BSs and the radar has to select a projection channel which minimizes degradation in its waveform, therefore increase its probability of target detection.

In figure 3(a), a scenario when dimN(**H**i) = 2 is considered. We demonstrate the results where radar waveform is projected onto five different BSs. Keeping in mind that in order to achieve a detection probability of 90%, 6 to 13 dB more gain is needed in SNR as compared to the orthogonal waveform. A results of less degradation of radar waveform and enhanced target detection performance with the minimum additional gain in SNR was attained. For instance, Algorithms 3 and 4 would select BS# number 5 because in this case NSP waveform requires least gain in SNR to attain a detection probability of 90% as equated to other BSs.

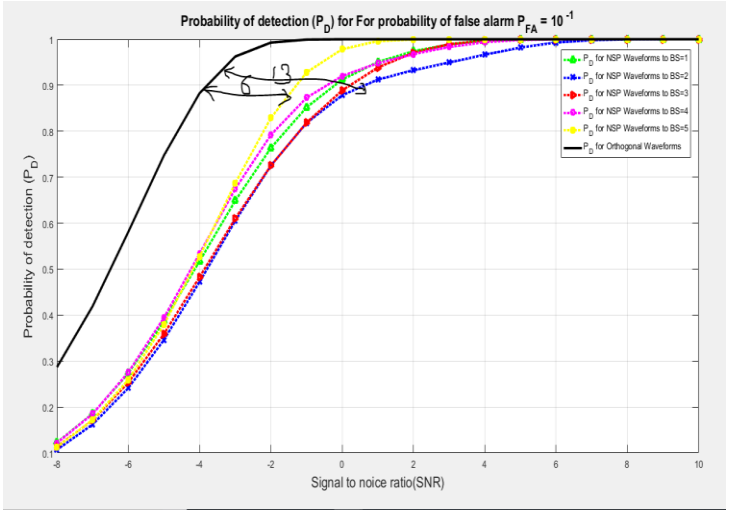

Figure3(a):Probability of detection when im[N(H_i)=2.

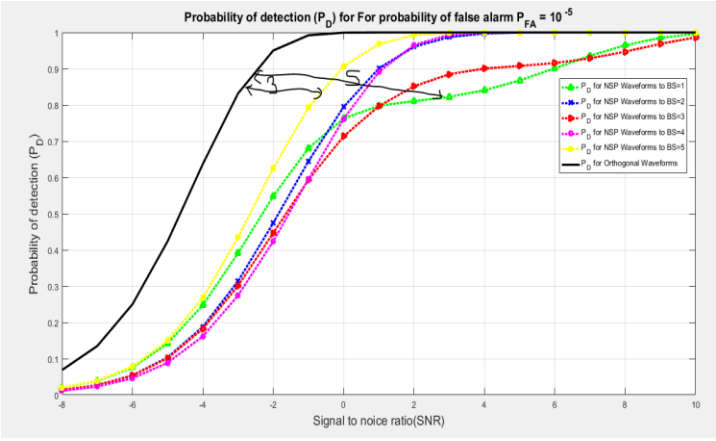

Figure3(b)Probability of detection when dim[N(H_i)=6.

In Figure 3(b), we consider the case when dimN(**H**i) = 6. Similar to figure 3(a) (detection results for five different NSP signals are shown) but in this case MIMO radar has a larger array of antennas as compared to scenario 1(a). In this scenario, in order to attain a detection probability of 90%, we need 3 to 5dB more gain in SNR as compared to the orthogonal waveform. Using Algorithms 3 and 4 results of less degradation of radar waveform and enhanced target detection performance with the minimum additional gain in SNR was attained. For instance, Algorithms 3 and 4 would select BS number 2 because in this case NSP waveform requires least gain in SNR to attain a detection probability of 90% as equated to the other BSs. The above two examples shows vividly the usefulness of Algorithms 3 and 4 in selecting best channel and henceforth enhance spectrum sharing.

4.1.1 Scenario 1(a)

We consider dimN(**H**i) = 2: Figure 4, shows variations of probability of detection P_D as a function of signal-to-noise ratio (SNR) for various values of probability of false alarm P_{FA}. We assess P_D versus P_{FA} values of 10^{-1}, 10^{-3}, 10^{-5} and 10^{-7} when the interference channel **H**i has dimensions 2 × 4, (radar has M = 4 antennas and the cellular communication network has $\mathcal{N}^{BS} = 2$ antennas), therefore we have a null-space dimension of 'dimN(**H**i) = 2'. More SNR for NSP is needed when we compare the detection performance of two waveforms to get a desired P_D for a fixed P_{FA} than orthogonal waveforms. For instance , in order to achieve $P_D = 0.9$, then rendering to Figure 4 we need 6 dB more gain in SNR for NSP waveform to get the same result produced by the orthogonal waveform.

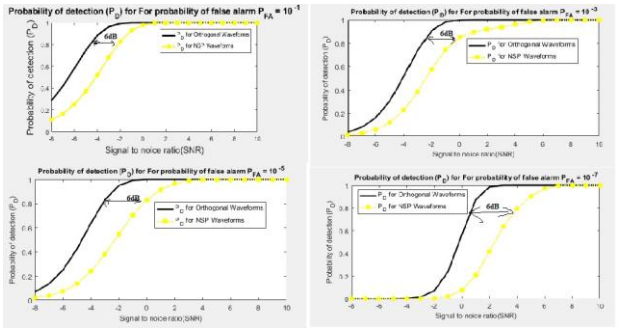

Figure 4:'Scenario 1(a): 'Scenario 1(a): dim[N(H_i)= 2: P_D as a function of SNR for various values of probability of false alarm PFA, i.e., $P_{FA} = 10^{-1}, 10^{-3}, 10^{-5}$ and 10^{-7}. The interference channel H_i has M = 4 antennas and the communication system has $\mathcal{N}^{BS} = 2$ antennas, therefore, we have a null-space dimension of 'dim[N(H_i)= 2'

4.1.2 Scenario 1(b)

In this scenario dimN(**H**i) = 6: In Figure 5 we do an analysis of P_D versus same values of P_{FA} but with interference channel **H**i having M = 8 antennas and the communication

system has $\mathcal{N}^{BS} = 2$ antennas, therefore ,we have a null-space dimension of 'dimN(**H**i) = 6'. Again, more SNR for NSP is needed when we compare the detection performance of two waveforms to get a desired P_D for a fixed P_{FA} than orthogonal waveforms.. For instance, let say we need P_D = 0.9, then according to Figure 5 we requisite 3.5 to 4.5dB extra gain in SNR for the NSP waveform to get the similar outcome produced by the orthogonal waveform.

4.1.3 Comparison of Case 1(a) and Case 1(b)

When SNR rises detection performance rises for both waveforms. But, comparing the two waveforms keeping SNR fixed, the orthogonal waveforms perform much better than the NSP waveform in detecting target. The season behind is: our transmitted waveforms are no longer orthogonal and we lose the advantages given by orthogonal waveforms when used in MIMO radars as discussed in subsection 1.B.6, however, zero-interference to the BS of interest was ensured, thus, sharing radar spectrum at an bigger cost of target detection in terms of SNR. In Scenario 1(a), in order to attain a preferred P_D for a fixed P_{FA} we requisite more SNR for NSP as equated to Scenario 1(b). This is because more radar antennas were used, while the antennas at the BS remain fixed in Scenario 1(b) which rises the dimension of the null space of the interference channel. This produces improved detection performance even for NSP waveform. Thus, in order to alleviate the effect of NSP on radar performance one way is to use a larger array at the radar transmitter.

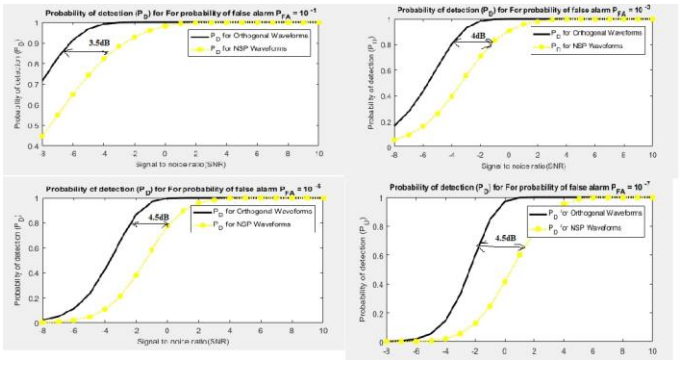

Figure 5: Scenario 1(a): 'Scenario 1(b): dim[N(H_i)= 6: P_D as a function of SNR for various values of probability of false alarm PFA, i.e., $P_{FA} = 10^{-1}, 10^{-3}, 10^{-5}$ and 10^{-7}. The interference channel H_i has M = 4 antennas and the communication system has $\mathcal{N}^{BS} = 2$antennas, thus, we have a null-space dimension of 'dim[N(H_i)= 6'.

4.2 Scenario-2 Analysis

Summarily, in this scenario at each run of Monte Carlo simulation K Rayleigh interference channels were generated, chain them into one interference channel with dimensions$K\mathcal{N}^{BS} \times M$, compute its null space and build corresponding projection matrix using Algorithm 6, execute projection of radar signal using Algorithm 5, transmit NSP signal, approximate parameters θ and α from the received signal, and compute the probability of detection for orthogonal and NSP waveforms.

In figure 6, we consider the case when the radar has a very large antenna array as equated to the combined antenna array of K BSs. In such a scenario, we have enough degrees of freedom at the radar for reliable target detection and concurrently nulling out interference to all the BSs present in the network. For instance, in Figure 6, we consider M = 100, K = 5, and $\mathcal{N}^{BS} = \{2, 4, 6, 8\}$ .We do an exploration of P_D versus PFA = 10^{-5} for the joined interference channel **H** having dimensions$K\mathcal{N}^{BS} \times M$,When we equate the detection performance of original waveform and NSP waveform onto the combined channel we footnote that for the aim of getting a desired PD for a fixed PFA more SNR for NSP is needed when we compare the detection performance of two waveforms to get a desired P_D for a fixed P_{FA} than orthogonal waveforms. For instance, let's say we need P_D = 0.95, then rendering to figure 6 we need 1, 2, 3.5, and 4.5 dB more gain in SNR for the NSP waveform when NBS is 2, 4, 6, and 8,respectively, to get the same outcome created by the orthogonal waveforms.

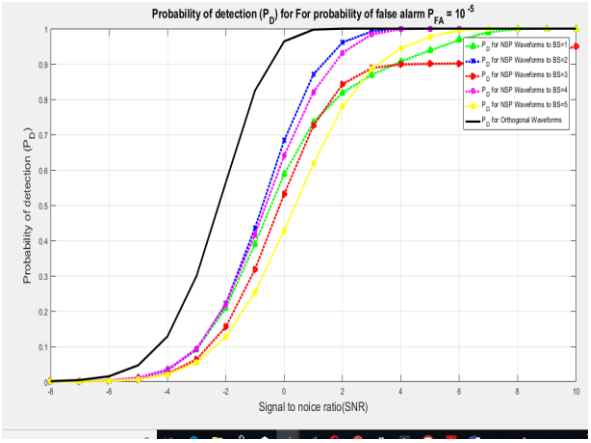

Figure 6: Scenario 2: P_D as a function of SNR for$P_{FA} = 10^{-5}$. The MIMO radar mitigates interference to all the BSs in the network. As an example, we consider M = 100 ,K= 5, and $\mathcal{N}^{BS} = \{2, 4, 6, 8\}$

5. CONCLUSION

Spectrum sharing is much anticipated to be the solution to the problem of increasing bandwidth demand in the future wireless communication (5G). The sharing of spectrum will help in many ways to make efficient use of the licensed spectrum and will henceforth save cost(s) and back-up the capacity increase in wireless communications. However, the spectrum sharing between radar and cellular communication is now getting an attention as one of the areas for spectrum frequency sharing in the future wireless communication (5G). In this paper, we examined spectrum

sharing scenario between MIMO radars and cellular communication network. The main focus was interference mitigation where by the radar signals were formed such that they do not cause interference to the cellular communication network. Using projection approach, the radar signals were projected onto the null space interference channel to a cellular communication system with many base stations and we evaluated the radar detection performance. We further impose different scenarios to formulate detection problem and deployed the MIMO radar system to decide about the presence of target when using orthogonal waveform and null-space projection waveforms. Spectrum sharing algorithms for various scenarios were proposed in which MIMO radar is sharing spectrum with cellular wireless communication network. The simulation results showed that the interferences were manageably mitigated.

REFERENCES

[1] M. J. Shundi and E. Mwangela, "A Review on Coordination Techniques for Licensed Spectrum Sharing in 5G Networks," vol. 8, no. 9, pp. 16–25, 2018.

[2] C. Yang, J. Li, M. Guizani, A. Anpalagan, and M. Elkashlan, "Advanced spectrum sharing in 5G cognitive heterogeneous networks," IEEE Wirel. Commun., vol. 23, no. 2, pp. 94–101, 2016.

[3] B. M. J. Marcus and D. Sc, "New Approaches to Private Sector Sharing of Federal Government Spectrum," no. June, 2009.

[4] M. Radmard, M. M. Chitgarha, M. Nazari Majd, and M. M. Nayebi, "Ambiguity function of MIMO radar with widely separated antennas," Proc. Int. Radar Symp., no. 1, 2014.

[5] N. Colon-Diaz, J. G. Metcalf, D. Janning, and B. Himed, "Mutual coupling analysis for colocated MIMO radar applications using CEM modeling," 2017 IEEE Radar Conf. RadarConf 2017, pp. 0441–0446, 2017.

[6] A. Nysaeter and H. Iwe, "Antenna Processing Optimization for a Colocated MIMO Radar," pp. 1–5, 2016.

[7] M. J. Shundi and G. G. Mihuba, "Improved Diagonal Loading for Robust Adaptive Beamforming Based On LS-CMA," vol. 6, no. 8, pp. 19–29, 2018.

[8] A. Khawar, A. Abdel-hadi, T. C. Clancy, and R. Mcgwier, "Beampattern Analysis for MIMO Radar and Telecommunication System Coexistence," no. 1, pp. 534–539, 2014.

[9] D. Tse, "Fundamentals of Wireless Communication 1," 2004.

[10] O. Font-Bach et al., "Experimental performance evaluation of a 5G spectrum sharing scenario based on field-measured channels," IEEE Int. Symp. Pers. Indoor Mob. Radio Commun. PIMRC, vol. 2015–Decem, pp. 856–861, 2015.

[11] J. A. Mahal, A. Khawar, A. Abdelhadi, T. C. Clancy, and I. T. Mar, "Radar Precoder Design for Spectral Coexistence with Coordinated Multi-point (CoMP) System," pp. 1–11.

[12] J. Kruys, P. Anker, and R. Schiphorst, "Spectrum sharing metrics," Info, vol. 16, no. 5, pp. 19–31, 2014.

[13] B. Wellenius and I. Neto, "The radio spectrum: Opportunities and challenges for the developing world," Info, vol. 8, no. 2, pp. 18–33, 2006.

[14] X. Chen and J. Huang, "Spatial Spectrum Access Game: Nash Equilibria and Distributed Learning," Proc. Thirteen. ACM Int. Symp. Mob. Ad Hoc Netw. Comput., pp. 205–214, 2012.

[15] S. Choi, H. Park, and T. Hwang, "Optimal beamforming and power allocation for sensing-based spectrum sharing in cognitive radio networks," IEEE Trans. Veh. Technol., vol. 63, no. 1, pp. 412–417, 2014.

[16] M. Sayed, M. Abdallah, K. Qaraqe, K. Tourki, and M. S. Alouini, "Joint opportunistic beam and spectrum selection schemes for spectrum sharing systems with limited feedback," IEEE Trans. Veh. Technol., vol. 63, no. 9, pp. 4408–4421, 2014.

[17] D. Trajkov, J. B. Evans, and J. A. Roberts, "Spectrum sharing for directional systems," p. 8–es, 2007.

[18] L. Anchora, M. Mezzavilla, L. Badia, and M. Zorzi, "Simulation models for the performance evaluation of spectrum sharing techniques in OFDMA networks," p. 249, 2011.

[19] M. Goldhamer and others, "Spectrum sharing between wireless systems," vol. 18, no. 5, pp. 1401–1412, 2007.

[20] N. Taramas, G. C. Alexandropoulos, and C. B. Papadias, "Opportunistic beamforming for secondary users in licensed shared access networks," ISCCSP 2014 - 2014 6th Int. Symp. Commun. Control Signal Process. Proc., pp. 526–529, 2014.

[21] I. Repository, "Network visualization : a review," vol. 2, no. 6, pp. 856–868, 2007.

[22] S. S. Bhat, R. M. Narayanan, and M. Rangaswamy, "Bandwidth sharing and scheduling for multimodal radar with communications and tracking," Proc. IEEE

Sens. Array Multichannel Signal Process. Work., pp. 233–236, 2012.

[23] R. Saruthirathanaworakun, J. M. Peha, and L. M. Correia, "Performance of data services in cellular networks sharing spectrum with a single rotating radar," 2012 IEEE Int. Symp. a World Wireless, Mob. Multimed. Networks, WoWMoM 2012 - Digit. Proc., 2012.

[24] S. Sodagari, A. Khawar, T. C. Clancy, and R. McGwier, "A projection based approach for radar and telecommunication systems coexistence," GLOBECOM - IEEE Glob. Telecommun. Conf., pp. 5010–5014, 2012.

[25] F. Paisana, J. P. Miranda, N. Marchetti, and L. A. Dasilva, "Database-aided sensing for radar bands," 2014 IEEE Int. Symp. Dyn. Spectr. Access Networks, DYSPAN 2014, pp. 1–6, 2014.

[26] H. Deng and B. Himed, "Interference mitigation processing for spectrum-sharing between radar and wireless communications systems," IEEE Trans. Aerosp. Electron. Syst., vol. 49, no. 3, pp. 1911–1919, 2013.

[27] A. Munari, N. Grosheva, L. Simić, and P. Mähönen, "Performance of Radar and Communication Networks Coexisting in Shared Spectrum Bands," pp. 1–8, 2019.

[28] J. A. Mahal, A. Khawar, A. Abdelhadi, and T. C. Clancy, "Spectral Coexistence of MIMO Radar and MIMO Cellular System," IEEE Trans. Aerosp. Electron. Syst., vol. 53, no. 2, pp. 655–668, 2017.

[29] J. H. Lim, D. W. Lim, B. L. Cheong, and M. S. Song, "Spectrum Sharing in Weather Radar Networked System: Design and Experimentation," IEEE Sens. J., vol. 19, no. 5, pp. 1720–1729, 2018.

[30] M. Hirzallah and T. Bose, "Steepest descent opportunistic MIMO radar: spectrum sharing design," Analog Integr. Circuits Signal Process., vol. 91, no. 2, pp. 227–237, 2017.

[31] A. Hatahet, A. Jain, and I. Technology, "Beamforming in LTE FDD for Multiple Antenna Systems Beamforming in LTE FDD for Multiple Antenna Systems."

[32] S. Kay, Fundamentals of Statistical Signal Processing: Detection Theory (Prentice Hall, 1998).

BIOGRAPHIES:

Michael Joseph Shundi: received his Bachelor of Engineering in Electronics & Telecommunications Engineering in 2009 from Dar es Salaam Institute of Technology, Tanzania. He is currently pursuing Master Degree in Information and Communication Engineering at the University of Science and Technology Beijing, China. His research areas include; Spectrum sharing, Radar systems, 5G Networks, and Computer Technologies. He is also an Instructor at Arusha Technical College, Tanzania

Ibrahim Iddi: is an Assistant Lecturer at Arusha Technical College, Tanzania. He pursued his Bachelor Degree at the University of Dar es Salaam, Tanzania. He did his Masters' Degree in Telecommunications Engineering at University of Dodoma, Tanzania. He is now pursuing PhD in Information and Communication Engineering at Beihang University, Beijing, China. His research areas includes; Radar systems, satellite communications, 5G Networks and Computer Systems.

Grace Gregory Mihuba received her Bachelor of Engineering in Electronics & Communications Engineering in 2013 from St. Joseph University in Tanzania, Tanzania. She is currently pursuing Master Degree in Information and Communication Engineering at the University of Science and Technology Beijing, China. Her research areas include; Telemedicine Systems design

Toshtemirov Adkhamjon received his Bachelor of Apparatus Constructing in Energetics in 2014 from the Fergana Polytechnic Institute, Uzbekistan. He is currently pursuing master degree in Information and Communication engineering at the University of Science and Technology Beijing, China. His research areas include; Block chain technology and 5G networks.